



Strong spatial population structure shapes the temporal coevolutionary dynamics of costly female preference and male display

Maximilian Tschol,^{1,2} Jane M. Reid,^{1,3} and Greta Bocedi¹

¹School of Biological Sciences, University of Aberdeen, Aberdeen AB24 2TZ, United Kingdom

²E-mail: m.tschol.18@abdn.ac.uk

³Centre for Biodiversity Dynamics, Institutt for Biologi, NTNU, Trondheim N-7491, Norway

Received August 27, 2020

Accepted November 26, 2021

Female mating preferences for exaggerated male display traits are commonplace. Yet, comprehensive understanding of the evolution and persistence of costly female preference through indirect (Fisherian) selection in finite populations requires some explanation for the persistence of additive genetic variance (V_a) underlying sexual traits, given that directional preference is expected to deplete V_a in display and hence halt preference evolution. However, the degree to which V_a , and hence preference-display coevolution, may be prolonged by spatially variable sexual selection arising solely from limited gene flow and genetic drift within spatially structured populations has not been examined. Our genetically and spatially explicit model shows that spatial population structure arising in an ecologically homogeneous environment can facilitate evolution and long-term persistence of costly preference given small subpopulations and low dispersal probabilities. Here, genetic drift initially creates spatial variation in female preference, leading to persistence of V_a in display through "migration-bias" of genotypes maladapted to emerging local sexual selection, thus fueling coevolution of costly preference and display. However, costs of sexual selection increased the probability of subpopulation extinction, limiting persistence of high preference-display genotypes. Understanding long-term dynamics of sexual selection systems therefore requires joint consideration of coevolution of sexual traits and metapopulation dynamics.

KEY WORDS: Dispersal, genetic drift, mating preference, sexual selection, spatial population structure.

Directional female mating preferences for elaborate and costly male display traits are widespread in nature (Andersson 1994; Wiens and Tuschhoff 2020). Explaining the evolution and long-term persistence of such female preferences and associated male displays has long challenged evolutionary biologists (Darwin 1871), especially when preferences are apparently costly with no clear direct fitness benefits (Pomiankowski 1987; Andersson 1994; Jennions and Petrie 1997; Friberg and Arnqvist 2003; Wong and Candolin 2005). Benefits of female preferences are then hypothesized to be indirect, stemming from genetic covariance between preference and male display that arises given initial additive genetic variance (V_a) in both traits and resulting non-random mating (i.e., "Fisherian sexual selection"; Fisher 1915; 1930; Lande 1981; Kirkpatrick 1982). Given such additive genetic (co)variances, male displays might be expected to evolve

such that survival costs (i.e., viability or natural selection; Lande 1981) are balanced by reproductive benefits through sexual selection.

Indeed, diverse models show that female preference can evolve via such indirect selection, depending on the strength of direct selection against preference and the shape of the variance-covariance matrix (G-matrix) for female preference and male display, and viability (Lande 1981; Kirkpatrick 1982; Kokko et al. 2002, 2006; Henshaw and Jones 2020). However, one persistent challenge is that directional sexual selection is expected to quickly deplete V_a in male display traits and associated fitness (the "Lek paradox"), eliminating indirect selection for costly female preference (Borgia 1979; Kirkpatrick and Ryan 1991). Identifying mechanisms that help maintain V_a over long biological timeframes therefore remains key to explaining the continued

expression of costly directional mating preference and resulting extraordinary phenotypic diversity (Mead and Arnold 2004; Tomkins et al. 2004; Kokko et al. 2006; Kotiaho et al. 2008; Radwan 2008; Prokuda and Roff 2014; Radwan et al. 2016; Lindsay et al. 2019).

Diverse mechanisms that could maintain V_a in male display have been proposed and tested (Radwan 2008; Bonilla et al. 2016; Radwan et al. 2016; Dugand et al. 2019). For example, V_a may be maintained by mutation-selection balance, whereby decreases due to sexual selection are compensated by sufficient frequency of new deleterious mutations (Iwasa et al. 1991; Pomiankowski et al. 1991), which could occur given a large enough mutational target (Pomiankowski and Møller 1995; Rowe and Houle 1996; Houle and Kondrashov 2002). Balancing selection may also maintain V_a through heterozygote advantage (Curtsinger and Heisler 1988; Fromhage et al. 2009), negative frequency dependence in host-parasite cycles (Hamilton and Zuk 1982), and antagonistic pleiotropy (Radwan et al. 2016; Li and Holman 2018), for example, stemming from antagonistic selection in different environments.

In addition, spatially variable selection has been widely suggested to maintain V_a given limited gene flow between diverged populations (Hedrick 1986; Kisdi 2001; Byers 2005; Gray and McKinnon 2007; McDonald and Yeaman 2018). Specifically, given local adaptation, immigrants to any focal subpopulation will likely be maladapted, causing deviations from current local optima in either direction, thereby increasing V_a in fitness (Lenormand 2002). Costly female preferences for local male displays could then be maintained by recurring immigration (Day 2000; Proulx 2001; Reinhold 2004). This mechanism could be commonplace if mating preferences and resulting sexual selection vary spatially (Payne and Krakauer 1997; Day 2000; Brooks 2002; Kingston et al. 2003; Chunco et al. 2007; Gray and McKinnon 2007; M'Gonigle et al. 2012; Wellenreuther et al. 2014; Ponkshe and Endler 2018; Dytham and Thom 2020). Indeed, several models have shown that evolution of divergent female preferences can cause spatially variable sexual selection, for example, given spatially varying natural selection on male display (Lande 1982; Day 2000), varying male dispersal depending on mating success (Payne and Krakauer 1997), and spatial variation in carrying capacity combined with mate-search costs in females (M'Gonigle et al. 2012).

However, spatially varying natural selection or ecology may not be necessary for spatial processes to facilitate evolution of costly female preferences. Rather, spatially divergent preferences might evolve simply given initially neutral spatial population structure, defined here as spatial genetic variation arising from population subdivision with limited gene flow, without any ecological heterogeneity. Lande (1981) and Kirkpatrick (1982) both highlighted the potential importance of genetic drift in initiat-

ing preference-display coevolution, and later models showed that drift can generate divergence in mating preferences along the line of equilibrium between two completely isolated populations (Tazzyman and Iwasa 2010), even when preferences are costly (Uyeda et al. 2009). However, most models assumed infinite population size and constant genetic (co)variances (Mead and Arnold 2004; Kuijper et al. 2012), thus ignoring stochastic effects arising in finite populations. Therefore, the potential consequences of limited gene flow in facilitating persistence of V_a underlying display and associated preference evolution over long biological timeframes remain largely unexplored. Yet, within spatially structured populations, gene flow and genetic drift are both prominent processes that could shape G-matrices of sexual traits (Guillaume and Whitlock 2007; Dytham and Thom 2020; Reid and Arcese 2020), and thereby modulate costly preference and display coevolution.

Furthermore, although sexual selection is predicted to cause male display phenotypes to diverge from naturally selected optima (Lande 1981), the population dynamic consequences of resulting increased male mortality are seldom explicitly considered (Tanaka 1996; Kokko and Brooks 2003; Martínez-Ruiz and Knell 2017). Strong sexual selection might increase risk of evolutionary “suicide” (Kokko and Brooks 2003), limiting population persistence and hence inevitably eliminating costly display and preference genotypes. Such extinction risk might be greatest in small populations, where genetic drift is most prevalent. Overall temporal dynamics of preference-display coevolution might then differ markedly between spatially structured populations and large panmictic populations, as are typically considered.

To test our hypothesis that genetic drift, coupled with limited gene flow, can facilitate evolution and persistence of costly female preference and costly male display over long timeframes, we built a spatially and genetically explicit individual-based model that allows genetic (co)variances of both traits and subpopulation extinction dynamics to arise from emerging spatial population structure. Specifically, we examine the consequences of dispersal probability and level of metapopulation subdivision for the temporal dynamics of preference and display coevolution and subpopulation extinction. We focus on temporal dynamics occurring over long biological timeframes, not specifically on evolutionary equilibria (stable states). Such transient persistence of preference-display co-evolution could still have considerable ecological and evolutionary consequences, even if V_a is ultimately completely depleted. We ask (1) whether dispersal among subpopulations can prolong the persistence of V_a in male display given uniform natural selection, and hence whether stochastic processes can be sufficient to fuel evolution and long-term persistence of costly female preference via indirect selection; (2) whether the degree of metapopulation subdivision interacts with dispersal to affect preference-display coevolution; (3)

whether the degree and temporal trajectory of divergence in sexual traits depend on the level of spatial population structure; and (4) whether increasing spatial population structure elevates the risk of subpopulation extinction due to sexual selection. Consequently, we highlight the roles that initially neutral genetic variation and limited gene flow could play in shaping temporal evolutionary dynamics of sexual selection in spatially structured populations.

Methods

We model a species inhabiting a square spatial grid where each cell contains a subpopulation connected by dispersal. We assume ecologically homogeneous space, where each cell has identical carrying capacity K . At each nonoverlapping generation, individuals undergo a lifecycle consisting of mating and reproduction, adult death, offspring viability selection, and density-dependent survival, followed by dispersal. All model variables and parameters are summarized in Table S1.

GENETIC ARCHITECTURE

We model a diploid additive genetic system with two autosomal traits: female preference (P) and male display (D). Each individual carries $L = 10$ diploid, physically unlinked loci underlying each trait (i.e., free recombination), with sex-limited phenotypic expression. Any genetic covariance between female and male traits arises from linkage disequilibrium generated by nonrandom mating. We assume a continuum-of-alleles model (Kimura 1965), with infinite potential alleles at each locus producing continuous distributions of effects. Initial allele values are independently sampled from a normal distribution with mean θ_z (denoting the trait's naturally selected optimum) and variance $\sigma_{\alpha,0}^2$ for both traits. Each individual's genotypic value (gP, gD) is the sum of its $2L$ allele values. Phenotypes (P and D) correspond to the genotypes (i.e., no environmental variance), except we set $D = 0$ if $gD < 0$, meaning that male phenotypic display cannot be negative (e.g., envisaged as male crest or tail length), whereas female preference can take any real number.

MATING AND REPRODUCTION

Starting each generation, each female chooses a mate from all N_{males} males present within her subpopulation according to her preference phenotype. Specifically, each male j has probability p_j of mating with female i , which depends on the strength of female i 's preference (P_i) and male j 's display (D_j) relative to the displays of all other males in the subpopulation (Lande 1981; Bocedi and Reid 2015):

$$p_j = \frac{e^{D_j P_i}}{\sum_{z=1}^{N_{\text{males}}} e^{D_z P_i}}. \quad (1)$$

We model a psychophysical preference function where negative and positive values of P represent preference for smaller and larger than average displays, respectively (Lande 1981). All females mate once, whereas males can mate multiple times or remain unmated. Each female then produces a number of offspring drawn from a Poisson distribution with mean $R = 4$, assuming a 1:1 primary sex ratio. For each locus, each offspring inherits a randomly selected allele from each parent. Each allele has mutation probability of $\mu = 5 \times 10^{-4}$ per generation. Mutational effects are sampled from a normal distribution with mean μ_m and variance σ_{α}^2 (Table S1).

SURVIVAL AND DISPERSAL

Offspring survival results from consecutive viability selection and density dependence. First, each offspring i experiences stabilizing selection around a naturally selected optimum phenotype, with viability v_i (Lande 1981; Bocedi and Reid 2015):

$$v_i = e^{\frac{-(z-\theta_z)^2}{2\omega_z^2}}, \quad (2)$$

where z denotes individual i 's phenotype (i.e., P or D), θ_z the trait's naturally selected optimum (constant $\theta_z = 0$ across subpopulations), and ω_z the strength of stabilizing selection (higher values give weaker selection). Any deviation from θ_z due to sexual selection decreases the individual's viability, imposing an absolute cost on preference or display. This may represent an energetic cost of male display (Basolo and Alcaraz 2003) or a "choosiness" cost of female preference (Jennions and Petrie 1997). As we set global optima, stabilizing selection on sexual traits acts similarly in all subpopulations. After viability selection, each offspring survives with density-dependent probability (ς):

$$\varsigma = \min\left(\frac{K}{N_{\text{offs}}}, 1\right), \quad (3)$$

where N_{offs} is the subpopulation total number of offspring. The relative contributions to mortality of selection versus density dependence thus depend on the distance of the subpopulation mean from the trait's naturally selected optimum and the local subpopulation density after selection.

Each offspring that survives viability selection and density-dependent mortality may disperse to a different subpopulation with probability d . Distance and direction for each dispersal event are drawn from negative exponential (mean = 1 cell) and uniform real (0-2 π) distributions, respectively, applied from a random starting point within the natal cell. If the destination falls outside the grid or within the current cell, distance and direction are resampled. This typically generates relatively short distance dispersal, with infrequent longer distance movements (Bocedi and Reid 2017).

SIMULATION EXPERIMENTS

We investigated effects of spatial population structure on coevolution of female preference and male display in two ways. First, we examined effects of dispersal among subpopulations by varying dispersal probability ($d = 5 \times 10^{-5}, 5 \times 10^{-4}, 5 \times 10^{-3}, 0.05$) within a metapopulation described by a 7×7 cell grid where each cell represents a subpopulation (49 cells, each with $K = 154$). Exploratory simulations showed that $d > 0.05$ generated dynamics indistinguishable from a single panmictic population. Second, for each value of d , we varied the level of population subdivision by changing the square cell grid to accommodate 9, 25, 49, 100, and 144 subpopulations of equal size ($K = 834, 300, 154, 75$, and 52, respectively, to reach an overall metapopulation size close to our panmictic control simulations). To evaluate effects of spatial population structure, we compared all scenarios to a single panmictic control population of 7500 individuals. This size was chosen to minimize effects of genetic drift while retaining reasonable computation time.

We assumed relatively weak stabilizing selection on female preference ($\omega^2_P = 100$), but strong stabilizing selection on male display ($\omega^2_D = 4$). Indirect selection favoring female preference evolution implies that mean P evolves to higher values than expected under mutation-(natural)selection-drift-migration balance. Accordingly, to distinguish effects of drift and indirect sexual selection, we ran simulations for each scenario of spatial population structure where all females mate randomly (i.e., no preference) but experience the same stabilizing selection on a neutral trait acting as a control phenotype.

We initialized each simulation by sampling individuals' alleles for each trait such that the traits' genotypic distributions had mean equal to zero and variance equal to 0.25. Each simulation was run for 250,000 generations, representing a long biological timeframe, and replicated 50 times. For each subpopulation, we extracted the mean trait genotypic values, genotypic variance, and the genetic correlation between preference and display at regular time intervals. We then calculated the grand mean across subpopulation genotypic means, variance, and genetic correlations for each replicate and time point (hereafter subpopulation grand mean, mean subpopulation V_a , and genetic correlation). We further report the standard deviation of subpopulation trait means per metapopulation as a measure of subpopulation divergence. At each recorded generation, we also extracted the percentage of subpopulations per metapopulation that were extinct. For all results, we report the median and central 95% interval across replicates. Finally, to reveal underlying mechanisms driving the persistence of costly preference, we quantified the contributions of dispersal and segregation to V_a in display. Quantitative genetic models of the maintenance of costly preference invoke mutation or dispersal that is biased away from the locally preferred male genotypes (Pomiankowski

et al. 1991; Day 2000). To test whether dispersal was biased in an analogous way, we quantified the degree of immigrant maladaptation resulting from spatially varying sexual selection (details in Fig. S5).

To test sensitivity to key parameters, we ran additional simulations where the naturally selected optimum of male display $\theta_D = 10$ (allowing females to prefer either bigger or smaller than optimal displays), with different strengths of stabilizing natural selection on male display ($\omega^2_D = 100$) or female preference ($\omega^2_P = 25, 400$), lower mutation probability ($\mu = 5 \times 10^{-6}$), or more loci underlying each trait ($L = 100$). We also ran simulations where all allelic values were initialized with zero for both traits to examine whether solely mutational input, alongside drift and spatial dynamics, could initiate preference-display coevolution.

Results

LOW DISPERSAL PROBABILITIES PROMOTE EVOLUTION OF COSTLY FEMALE PREFERENCES

Compared to a single panmictic population, simply restricting dispersal probability d , and hence generating neutral spatial population structure, readily led to ongoing evolution of costly female preference and male display over long biological timeframes (Fig. 1). The magnitudes of these effects depended on the value of d . Given low values ($d < 5 \times 10^{-2}$), mean subpopulation female preference initially increased away from the naturally selected optimum of no preference (Fig. 1A). This increase in preference was mirrored by increasing male display (Fig. 1B). Exaggeration of both traits proceeded faster given $d = 5 \times 10^{-3}$, reaching maximum mean values within the initial 10,000 generations, and occurred more slowly given $d = 5 \times 10^{-4}$ (Fig. 1A, B). Eventually, after 250,000 generations, costly female preference only persisted at very low dispersal probability ($d = 5 \times 10^{-4}$). Depletion of V_a in both traits was initially faster given lower d ; however, the greatest V_a in display remained given dispersal probability $d = 5 \times 10^{-4}$ (Fig. 1D).

A positive genetic correlation between preference and display initially arose given $d > 5 \times 10^{-4}$ and peaked within the first 2000 generations before gradually decreasing to zero (Fig. 1E). However, given $d = 5 \times 10^{-4}$, a small positive genetic correlation persisted throughout the simulated period (Fig. 1E). In comparison, in control simulations with random mating, the distributions of genetic correlations were centered at zero, independent of dispersal probability (Fig. S1). Further, the distribution of subpopulation grand mean trait values was centered on the naturally selected optima. The difference between the main and control simulations (i.e., with and without sexual selection) suggests that indirect selection (in addition to drift) shaped preference evolution given preferential mating (Fig. S1).

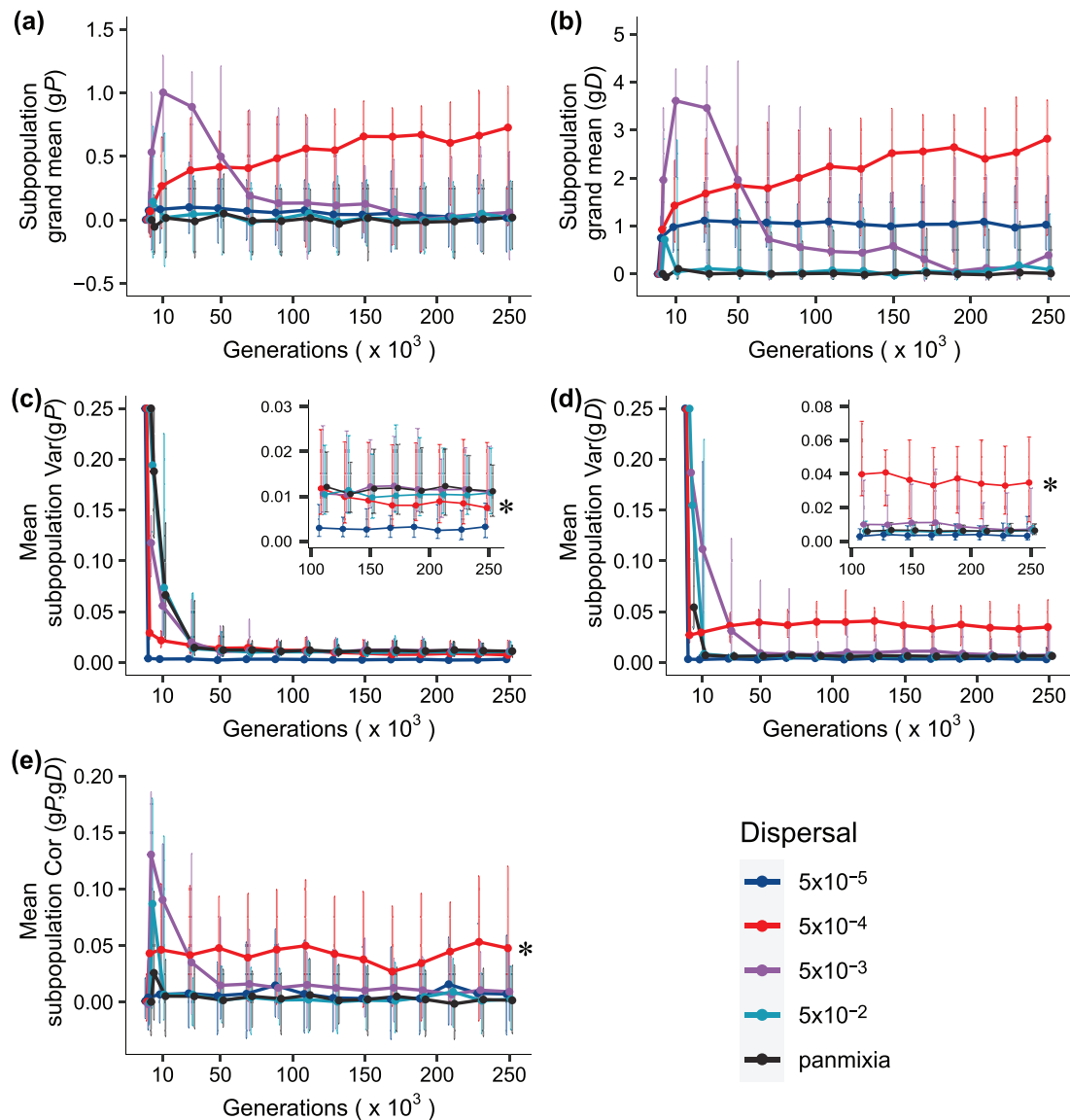


Figure 1. Coevolution of costly female preference and male display over 250,000 generations in metapopulations comprising 49 subpopulations given different dispersal probabilities (d). (A) Subpopulation grand mean preference genotype gP ; (B) subpopulation grand mean display genotype gD ; (C, D) mean subpopulation additive genetic variance (V_a) in gP and gD , where the insets zoom-in on the last 150,000 generations by changing the limits of the x- and y-axis to aid visualization; (F) mean subpopulation genetic correlation of preference and display $\text{Cor}(gP, gD)$. In all panels, points and solid lines indicate the median across 50 replicate simulations, and bars indicate the central 95% interval across replicates. Data are shown initially at generation 0, 2000, 10,000, and at intervals of 20,000 generations thereafter. Points are horizontally jittered to improve readability. Other parameters: $\omega^2_P = 100$ and $\omega^2_D = 4$. Asterisk (*) indicates long-term transient dynamics.

Further analyses showed that dispersal between subpopulations was the largest source of V_a in male display (Fig. S4). In simulations where costly preference persisted, male immigrants were on average maladapted to the sexually selected environment at their destination. Gene flow was therefore biased away from locally preferred male phenotypes (i.e., “migration bias”; Fig. S5).

Both short- and long-term persistence of female preference and male display, and hence the form of transient dynam-

ics, depended on the strength of selection against preference (Fig. S6). Stronger selection ($\omega^2_P = 25$) prevented preference evolution irrespective of d . Conversely, weaker selection ($\omega^2_P = 400$) allowed transient increases in subpopulation grand mean preference even given $d = 0.05$ (Fig. S6). Under weaker negative natural selection on male display ($\omega^2_D = 100$), display generally evolved to higher values compared to the main simulations (Fig. S8). Subpopulation grand mean preference and display

showed pronounced fluctuations across generations given $d < 5 \times 10^{-4}$, where preferences gradually changed from positive to negative, with corresponding responses in display (Fig. S8). Allowing evolution of either positive or negative male display by setting $\theta_D = 10$ led to higher V_a in display at $d = 5 \times 10^{-4}$, but preference and display evolution was otherwise equivalent to the main simulations (Fig. S10).

Results remained qualitatively similar given $L = 100$ loci underlying preference and display (Figs. S12 and S13). Lower mutation rate ($\mu = 5 \times 10^{-6}$) resulted in transient dynamics that were qualitatively similar to the main simulations, but complete depletion of V_a ultimately occurred within the simulated time period for all values of d (Fig. S15). Further, presence or absence of initial standing genetic variation in preference and display did not affect system state after 250,000 generations with $\mu = 5 \times 10^{-4}$ (Fig. S17). However, with lower mutation rates ($\mu < 5 \times 10^{-4}$), solely mutational input was not sufficient to initiate preference-display coevolution.

METAPOPULATION SUBDIVISION AND DISPERSAL INTERACT IN DETERMINING PREFERENCE-DISPLAY COEVOLUTION

Increasing or decreasing the number of subpopulations (i.e., metapopulation subdivision) altered the evolution and persistence of female preference and male display depending on dispersal probability (Figs. 2A, B and S19-S22). The main effect was increasing long-term subpopulation grand mean preference and display with increasing metapopulation subdivision given $d = 5 \times 10^{-3}$. In contrast, trait means decreased given $d = 5 \times 10^{-4}$, and even turned negative given $d = 5 \times 10^{-5}$ (Fig. 2A, B). V_a in preference generally increased with higher dispersal probability and lower metapopulation subdivision. In contrast, V_a in display was greatest at $d = 5 \times 10^{-4}$ and 5×10^{-3} , and given intermediate and high levels of metapopulation subdivision, respectively (Fig. 2C, D). Intermediate dispersal therefore counteracted the otherwise rapid depletion of V_a in highly structured populations, and increased V_a in display further compared to the panmictic case by preventing spatial homogenization of female preferences. Under random mating, subpopulation grand trait means remained at their naturally selected optima independently of metapopulation subdivision (Fig. S2). Further, greater V_a in display remained at $d = 5 \times 10^{-4}$ and 5×10^{-3} given sexual selection than under random mating (Fig. S2).

EFFECT OF SPATIAL POPULATION STRUCTURE ON SUBPOPULATION DIVERGENCE

The levels of dispersal and metapopulation subdivision influenced the build-up and persistence of divergence in preference and display among subpopulations (Fig. 3). Under intermediate metapopulation subdivision (49 subpopulations), the lowest dis-

persal probability ($d = 5 \times 10^{-5}$) resulted in high spatial differentiation in mean preference and display phenotypes across 250,000 generations, whereas $d \geq 5 \times 10^{-4}$ led to short transient differentiation followed by subsequent homogenization. Homogenization occurred faster, and was complete across subpopulations, with higher d (Fig. 3A, B) and lower metapopulation subdivision (Fig. S23). However, with $d = 5 \times 10^{-4}$ and high metapopulation subdivision, homogenization proceeded very slowly, leaving substantial differentiation even after 250,000 generations (Figs. 3C, D and S23). Population differentiation in preference generally increased with increasing subdivision, whereas differentiation in display was highest at intermediate subdivision (Fig. 3C, D). In contrast, simulations with random mating (i.e., no sexual selection) showed less population differentiation, especially in male display (Fig. S3).

Weaker direct selection against male display resulted in higher and fluctuating population differentiation in display given $d \leq 5 \times 10^{-4}$, but faster homogenization given $d > 5 \times 10^{-4}$ (Fig. S9). Setting optimal display phenotype $\theta_D = 10$ resulted in greater population differentiation in both preference and display, because preference-display coevolution proceeded toward both smaller and larger than optimal display, depending on the subpopulation (Fig. S11). The degree of population differentiation remained similar with $L = 100$ loci underlying the traits (Fig. S14).

INCREASING SPATIAL POPULATION STRUCTURE LEADS TO SUBPOPULATION EXTINCTION VIA SEXUAL SELECTION

Evolution of mating preference (i.e., sexual selection) led to subpopulation extinction events to degrees that depended on spatial population structure (Fig. 4). With sexual selection, some subpopulation extinction occurred given $d < 5 \times 10^{-2}$ and metapopulation subdivision > 25 subpopulations (Fig. 4). Unsurprisingly, increasing subdivision (i.e., decreasing subpopulation size) generally increased the proportion of subpopulations that went extinct (Fig. 4), occasionally resulting in extinction of entire metapopulations (Fig. S24). In contrast, no extinctions occurred with random mating, indicating that extinctions were driven by sexual selection.

Discussion

Previous stochastic models of coevolving female preference and male display provide important insights into interactions between sexual selection and genetic drift (Uyeda et al. 2009; Tazzyman and Iwasa 2010). These studies demonstrate diversification of mating preferences under drift and examine the consequences for evolution of preferred traits in the absence of gene flow. Here, we extend these concepts to examine the combined effects of genetic

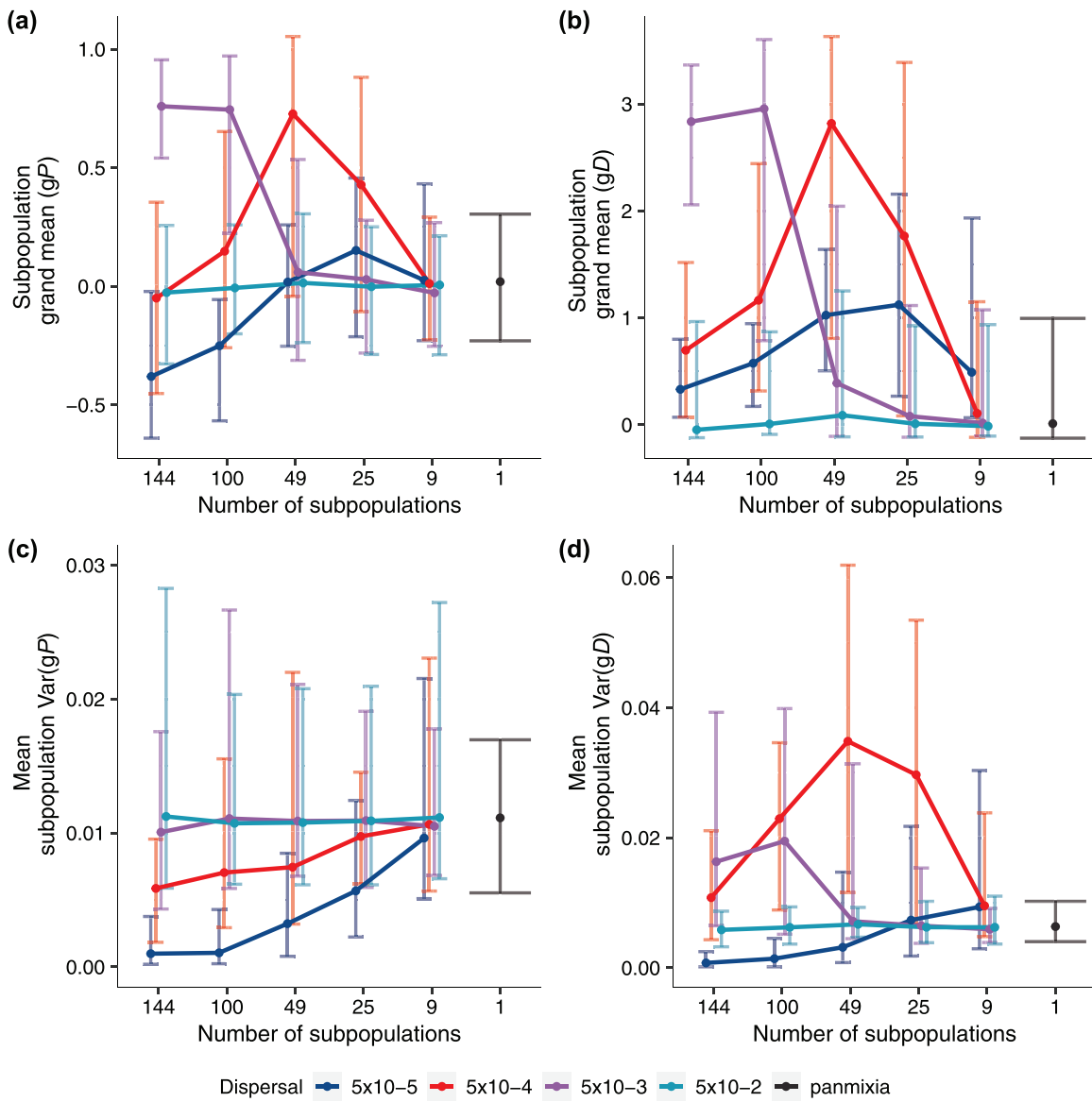


Figure 2. Effect of metapopulation subdivision (number of subpopulations) on the coevolution of costly female preference and male display, given different dispersal probabilities. (A) Subpopulation grand mean preference genotype gP ; (B) subpopulation grand mean display genotype gD ; (C, D) mean subpopulation additive genetic variance (V_a) in gP and gD . In all panels, points and solid lines indicate the median across 50 replicate simulations at generation 250,000, and bars indicate the central 95% interval across replicates. Points are horizontally jittered to improve readability. Other parameters: $\omega^2_P = 100$ and $\omega^2_D = 4$.

drift and dispersal in shaping preference-display coevolution in a metapopulation context within an ecologically homogeneous environment. As in previous models that did not include dispersal (Uyeda et al. 2009; Tazzyman and Iwasa 2010), the combination of drift and dispersal acting within small subpopulations caused preference to evolve to different points around a line of quasi-equilibrium in the preference-display genotypic space (Fig. S26). Low dispersal probabilities among subpopulations together with drift-induced female preference evolution created spatially variable sexual selection. Subsequent immigration of male genotypes that were maladapted to the local sexually selected environment

then led to a “migration bias” (Day 2000) that created V_a in male display. Consequently, females exhibiting mating preference continued to produce more attractive (fitter) sons, thereby fueling persistence of costly female preference across very long biological timeframes. Hence, initially neutral spatial population structure prolonged the persistence of V_a in male display compared to a panmictic population of identical overall size. However, these long transient dynamics of display and preference occurred only under a narrow range of low dispersal probabilities. Drift-induced evolution of costly female preference and costly male display was notably also associated with increased subpopulation extinction.

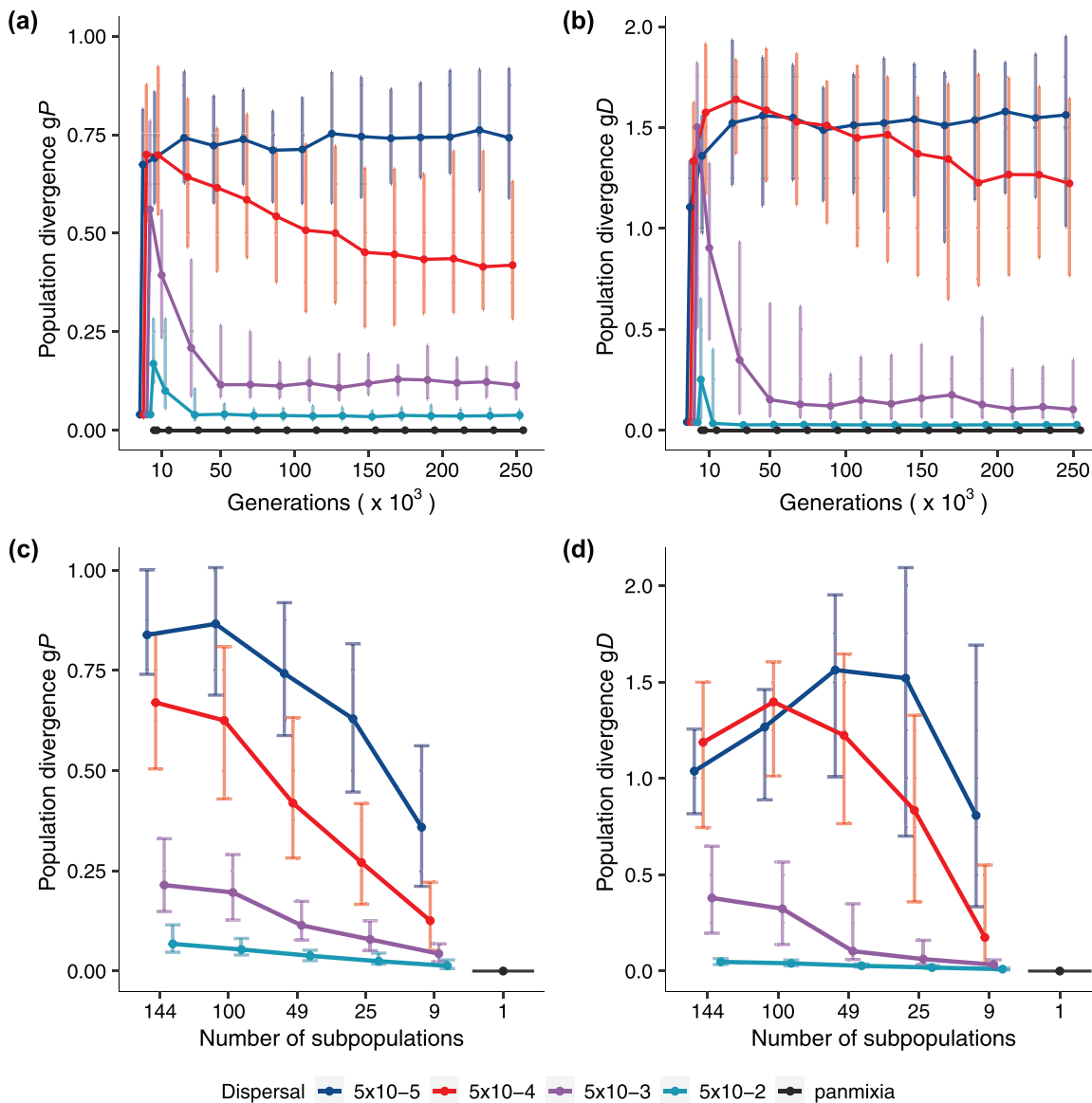


Figure 3. Population divergence in female preference genotype gP and male display genotype gD (A, B) over 250,000 generations and (C, D) at different levels of metapopulation subdivision (number of subpopulations) as a function of dispersal probability. Subpopulation divergence is measured as standard deviation of the subpopulation trait means across a metapopulation. Panels A and B consider metapopulations composed of 49 subpopulations and data are shown initially at generation 0, 2000, 10,000, and at intervals of 20,000 generations thereafter. Panels C and D show results at generation 250,000. In all panels, points and solid lines indicate the median across 50 replicate simulations, and bars indicate the central 95% interval across replicates. Points are horizontally jittered to improve readability. Other parameters: $\omega^2_P = 100$ and $\omega^2_D = 4$.

Our work further emphasizes the need to consider sexual selection in a spatially explicit ecological context to understand the evolution and persistence of sexual traits (Payne and Krakauer 1997; Day 2000; M'Gonigle et al. 2012). A recent study examined effects of population fragmentation on the diversity of individual identity signals under sexual selection, and found that global signal diversity increased by 10–15% in fragmented versus unfragmented habitat (Dytham and Thom 2020). Our results similarly suggest that fragmentation (here represented by strong

spatial structure) elevates genetic variation in male sexual signals and extensively prolongs the persistence of costly female preference. This raises the interesting empirical question of whether ongoing anthropogenic habitat fragmentation might ultimately elevate evolution and differentiation in species' sexually selected traits. Most empirical evidence of sexual trait differentiation as a consequence of habitat fragmentation relates to alteration of biotic and abiotic environments, such as changes in predation pressures or water turbidity (Giery et al. 2015; Giery and Layman

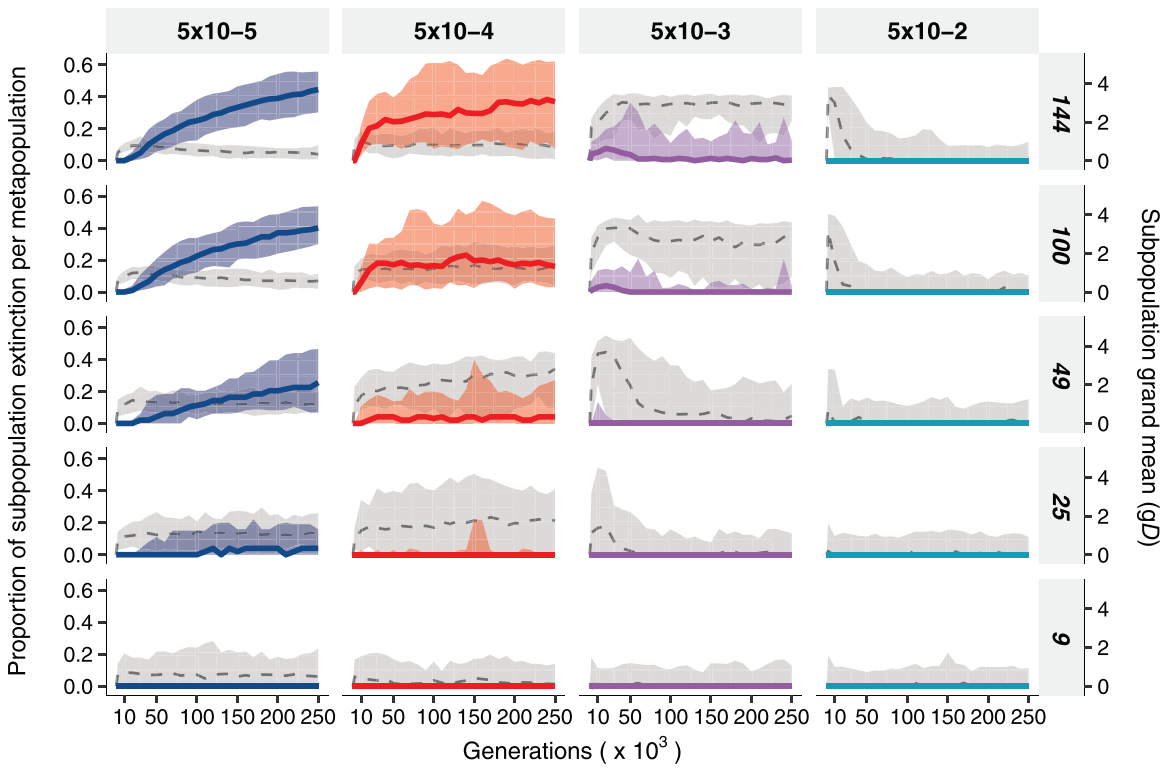


Figure 4. Proportion of subpopulations that went extinct (left y-axis) and male display evolution (right y-axis) over 250,000 generations, across different dispersal probabilities and levels of metapopulation subdivision. Colors and solid lines indicate population extinction, whereas dashed lines and gray shading refer to subpopulation grand mean display genotype gD . Lines indicate the median across 50 replicate simulations, and shading indicates the central 95% interval across replicates. Gray panels indicate different simulation scenarios of spatial population structure (x-axis: dispersal probabilities; y-axis: metapopulation subdivision).

2015; Zastavniouk et al. 2017). Yet, population differentiation in mating preferences that is not clearly associated with such environmental changes could indicate that the genetic consequences of habitat fragmentation have fueled preference evolution. Interestingly, increasing habitat fragmentation may increase costs of dispersal (Bonte et al. 2012; Cote et al. 2017), selecting against it and thereby facilitating preference-display coevolutionary dynamics under low dispersal.

In our model, greatest V_a in male display persisted over long timeframes given low dispersal probabilities ($d = 5 \times 10^{-4}$ and 5×10^{-3}). We showed that dispersal between subpopulations is the main cause, with very low contribution from mutation and segregation (Fig. S4). This indicates that prolonged persistence of V_a is tightly linked to the level of subpopulation differentiation in display. Although high metapopulation subdivision promoted differentiation, such systems require more dispersal to counteract rapid depletion of V_a due to smaller subpopulations size. Ultimately, because our model allowed the source of spatial variation in sexual selection (i.e., female preference) to evolve, homogenization of female preference with increasing dispersal generally caused depletion of V_a in display.

Our results generally concur with recent findings that Fisherian sexual selection alone cannot maintain population divergence given substantial gene flow (Servedio and Bürger 2014, 2015). Servedio and Bürger (2014) examined divergence in a preference and a male display trait in a two-locus haploid model, and found that increasing sexual selection inhibited differentiation between populations connected by gene flow due to limited divergence in preference. When female preference could evolve, weaker preference alleles successfully invaded until preference disappeared. However, at low dispersal, our analysis of quantitative variation underlying preference and display showed that gene flow played a crucial role in generating a positive genetic correlation across initial generations, and divergence in sexual traits often persisted for substantial periods of time in structured populations. Similarly, M'Gonigle et al. (2012) showed how variation in local carrying capacity combined with mate-search-dependent costs to females can facilitate prolonged persistence of ecologically equivalent mating types. In our model, similar persistence of variation in preference and display emerged with neither variation in local carrying capacity nor mate-search costs.

Drift-induced evolution of female preference has been shown to increase differentiation between populations (Uyeda et al. 2009; Tazzyman and Iwasa 2010) and is expected to help initiate Fisherian preference-display coevolution (Lande 1981). However, genetic drift is higher in small populations, which also have higher extinction risk. Our simulations highlight this balance for small and fragmented populations: genetic drift and little dispersal promote evolution of female preference for costly male display, but such populations are also prone to extinction, likely because of increased mortality due to expression of costly male traits (Kokko and Brooks 2003; Martínez-Ruiz and Knell 2017). Further, under some scenarios, specifically with weak stabilizing natural selection on preference and/or display, subpopulation extinctions can lead to rapid shifts in the metapopulation trait means that somewhat resemble previously described cycles of preference-display coevolution (Iwasa and Pomiankowski 1995; Kuijper et al. 2012). In our case, trait changes are apparently driven by the combination of weak stabilizing selection leading to runaway coevolution of the sexual traits, and associated extinction-recolonization dynamics (cf. Figs. S8 and S25). Interestingly, some degree of population extinction may contribute positively to the persistence of costly preference because almost extinct populations will generate fewer migrants, contributing to biased dispersal toward individuals with lower display values than the metapopulation average (Fig. S27). This raises interesting questions regarding potential interactions between metapopulation dynamics and maintenance of V_a for sexual traits, which remain to be explored.

The observed local extinction dynamics presumably depend on assumptions regarding the strength and form of natural selection on display. We modeled strong enough natural selection to outweigh genetic drift even in highly structured populations, thereby highlighting evolution of costly display in response to sexual selection. We assumed natural selection to be relative to a global phenotypic optimum, independently from local male display genotypes and density (Reznick 2016; De Lisle and Svensson 2017). Alternative modes of selection would likely alter outcomes. For example, frequency-dependent, or soft rather than hard, natural selection may reduce the costs of display locally, reducing male mortality and allowing subpopulations to diverge further compared to a global phenotypic optimum, potentially increasing persistence of V_a and of entire (meta)populations. Conversely, higher population differentiation might increase the costs of display disproportionately for immigrant males if selection acts relative to the local mean phenotype, potentially limiting the persistence of V_a by reducing gene flow between subpopulations (Gosden et al. 2015). Although our assumption about the form and strength of natural selection may particularly promote male mortality, this effect is likely counteracted by our assumption that all local females could reproduce with a single surviving male.

Allee effects arising from limited mate availability may otherwise be expected to further increase population extinction risk (Shaw and Kokko 2014). Future studies could investigate different forms of natural selection on display and link costs of female preferences, in terms of missed reproduction opportunities, to local male density. Similarly, alternative assumptions regarding individual dispersal provide avenues for future investigations. Dispersal decisions and costs are complex, and often depend on individual phenotype and/or local competition (Bowler and Benton 2005). Introducing such complexity could cause a migration bias, for example, when males with larger displays pay proportionally higher costs of dispersing.

Overall, our model demonstrates that purely spatial population structure, arising from population subdivision and restricted ranges of limited dispersal, can fuel costly preference-display evolution and allow V_a in display to persist over long biological timescales without invoking spatially variable natural selection on display or unrealistically high mutation rates. Yet, we show that populations with extreme preference-display genotypes experience evolutionary suicide, driving long-term extinction-recolonization dynamics. These analyses should inspire future investigations of preference-display coevolutionary dynamics across more complex spatial and fitness landscapes.

ACKNOWLEDGMENTS

We thank B. Willink Castro and W. R. Tschohl for their helpful insights throughout the project. MT and GB were funded by the Royal Society through GB's University Research Fellowship (UF160614) and Research Fellows Enhancement Award (RGFEA180184). JMR was supported by Research Council of Norway (SFF-III, project 223257) and NTNU. Computer simulations were performed using the Maxwell Computing Cluster at the University of Aberdeen.

AUTHOR CONTRIBUTIONS

MT, JR, and GB conceived and designed the study. MT and GB designed and analyzed the model. MT wrote the first draft of the manuscript and all authors contributed substantially to revisions.

CONFLICT OF INTEREST

The authors declare no conflict of interest.

DATA ARCHIVING

Source code has been deposited on <https://doi.org/10.5281/zenodo.5781486>.

LITERATURE CITED

Andersson, M. B. 1994. Sexual selection. Princeton Univ. Press, Princeton, NJ.
 Basolo, A. L., and G. Alcaraz. 2003. The turn of the sword: length increases male swimming costs in swordtails. *Proc. R. Soc. B Biol. Sci.* 270:1631–1636.

Bocedi, G., and J. M. Reid. 2015. Evolution of female multiple mating: a quantitative model of the “sexually selected sperm” hypothesis. *Evolution* 69:39–58.

———. 2017. Feed-backs among inbreeding, inbreeding depression in sperm traits, and sperm competition can drive evolution of costly polyandry. *Evolution* 71:2786–2802.

Bonilla, M. M., J. A. Zeh, and D. W. Zeh. 2016. An epigenetic resolution of the lek paradox. *Bioessays* 38:355–366.

Bonte, D., H. van Dyck, J. M. Bullock, A. Coulon, M. Delgado, M. Gibbs, V. Lehouck, E. Matthysen, K. Mustin, M. Saastamoinen, et al. 2012. Costs of dispersal. *Biol. Rev. Camb. Philos. Soc.* 87:290–312.

Borgia, G. 1979. Sexual selection and the evolution of mating systems. Pp. 19–80 in M. S. Blum and N. A. Blum, eds. *Sexual selection and reproductive competition in insects*. Academic Press, New York.

Bowler, D. E., and T. G. Benton. 2005. Causes and consequences of animal dispersal strategies: relating individual behaviour to spatial dynamics. *Biol. Rev.* 80:205–225.

Brooks, R. 2002. Variation in female mate choice within guppy populations: population divergence, multiple ornaments and the maintenance of polymorphism. *Genetica* 116:343–358.

Byers, D. L. 2005. Evolution in heterogeneous environments and the potential of maintenance of genetic variation in traits of adaptive significance. Pp. 107–124 in R. Mauricio, ed. *Genetics of adaptation*. Georgia genetics review III. Springer-Verlag, Berlin/Heidelberg.

Chunco, A. J., J. S. McKinnon, and M. R. Servedio. 2007. Microhabitat variation and sexual selection can maintain male color polymorphisms. *Evolution* 61:2504–2515.

Cote, J., E. Bestion, S. Jacob, J. Travis, D. Legrand, and M. Baguette. 2017. Evolution of dispersal strategies and dispersal syndromes in fragmented landscapes. *Ecoigraphy* 40:56–73.

Curtsinger, J. W., and I. L. Heisler. 1988. A diploid “sexy son” model. *Am. Nat.* 132:437–453.

Darwin, C. 1871. *The descent of man and selection in relation to sex*. John Murray, Lond.

Day, T. 2000. Sexual selection and the evolution of costly female preferences: spatial effects. *Evolution* 54:715–730.

De Lisle, S. P., and E. I. Svensson. 2017. On the standardization of fitness and traits in comparative studies of phenotypic selection. *Evolution* 71:2313–2326.

Dugand, R. J., J. L. Tomkins, and W. J. Kennington. 2019. Molecular evidence supports a genic capture resolution of the lek paradox. *Nat. Commun.* 10:1359.

Dytham, C., and M. D. F. Thom. 2020. Population fragmentation drives up genetic diversity in signals of individual identity. *Oikos* 129:526–532.

Fisher, R. A. 1915. The evolution of sexual preference. *Eugen. Rev.* 7:184–192.

———. 1930. *The genetical theory of natural selection*. Clarendon Press, Oxford, U.K.

Friberg, U., and G. Arnqvist. 2003. Fitness effects of female mate choice: preferred males are detrimental for *Drosophila melanogaster* females. *J. Evol. Biol.* 16:797–811.

Fromhage, L., H. Kokko, and J. M. Reid. 2009. Evolution of mate choice for genome-wide heterozygosity. *Evolution* 63:684–694.

Giery, S. T., and C. A. Layman. 2015. Interpopulation variation in a condition-dependent signal: predation regime affects signal intensity and reliability. *Am. Nat.* 186:187–195.

Giery, S. T., C. A. Layman, and R. B. Langerhans. 2015. Anthropogenic ecosystem fragmentation drives shared and unique patterns of sexual signal divergence among three species of Bahamian mosquitofish. *Evol. Appl.* 8:679–691.

Gosden, T. P., J. T. Waller, and E. I. Svensson. 2015. Asymmetric isolating barriers between different microclimatic environments caused by low immigrant survival. *Proc. R. Soc. B Biol. Sci.* 282:20142459.

Gray, S. M., and J. S. McKinnon. 2007. Linking color polymorphism maintenance and speciation. *Trends Ecol. Evol.* 22:71–79.

Guillaume, F., and M. C. Whitlock. 2007. Effects of migration on the genetic covariance matrix. *Evolution* 61:2398–2409.

Hamilton, W. D., and M. Zuk. 1982. Heritable true fitness and bright birds: a role for parasites? *Science* 218:384–387.

Hedrick, P. W. 1986. Genetic polymorphism in heterogenous environments: a decade later. *Annu. Rev. Ecol. Evol. Syst.* 17:535–566.

Henshaw, J. M., and A. G. Jones. 2020. Fisher’s lost model of runaway sexual selection. *Evolution* 74:487–494.

Houle, D., and A. S. Kondrashov. 2002. Coevolution of costly mate choice and condition-dependent display of good genes. *Proc. R. Soc. B Biol. Sci.* 269:97–104.

Iwasa, Y., and A. Pomiankowski. 1995. Continual change in mate preferences. *Nature* 377:420–422.

Iwasa, Y., A. Pomiankowski, and S. Nee. 1991. The evolution of costly mate preferences II. The “Handicap” principle. *Evolution* 45:1431–1442.

Jennions, M. D., and M. Petrie. 1997. Variation in mate choice and mating preferences: a review of causes and consequences. *Biol. Rev. Camb. Philos. Soc.* 72:283–327.

Kimura, M. 1965. A stochastic model concerning the maintenance of genetic variability in quantitative characters. *Proc. Natl. Acad. Sci. USA* 54:731–736.

Kingston, J. J., G. G. Rosenthal, and M. J. Ryan. 2003. The role of sexual selection in maintaining a colour polymorphism in the pygmy swordtail, *Xiphophorus pygmaeus*. *Anim. Behav.* 65:735–743.

Kirkpatrick, M. 1982. Sexual selection and the evolution of female choice. *Evolution* 36:1–12.

Kirkpatrick, M., and M. J. Ryan. 1991. The evolution of mating preferences and the paradox of the lek. *Nature* 350:33–38.

Kisdi, E. 2001. Long-term adaptive diversity in Levene-type models. *Evol. Ecol. Res.* 3:721–727.

Kokko, H., and R. Brooks. 2003. Sexy to die for? Sexual selection and the risk of extinction. *Ann. Zool. Fenn.* 40:207–219.

Kokko, H., R. Brooks, J. M. McNamara, and A. I. Houston. 2002. The sexual selection continuum. *Proc. R. Soc. B Biol. Sci.* 269:1331–1340.

Kokko, H., M. D. Jennions, and R. Brooks. 2006. Unifying and testing models of sexual selection. *Annu. Rev. Ecol. Evol. Syst.* 37:43–66.

Kotiaho, J. S., N. R. LeBas, M. Puurinen, and J. L. Tomkins. 2008. On the resolution of the lek paradox. *Trends Ecol. Evol.* 23:1–3.

Kuijper, B., I. Pen, and F. J. Weissling. 2012. A guide to sexual selection theory. *Annu. Rev. Ecol. Evol. Syst.* 43:287–311.

Lande, R. 1981. Models of speciation by sexual selection on polygenic traits. *Proc. Natl. Acad. Sci. USA* 78:3721–3725.

———. 1982. Rapid origin of sexual isolation and character divergence in a cline. *Evolution* 36:213–223.

Lenormand, T. 2002. Gene flow and the limits to natural selection. *Trends Ecol. Evol.* 17:183–189.

Li, X.-Y., and L. Holman. 2018. Evolution of female choice under intralocus sexual conflict and genotype-by-environment interactions. *Philos. Trans. R. Soc. Lond. B Biol. Sci.* 373:20170425.

Lindsay, W. R., S. Andersson, B. Bererhi, J. Höglund, A. Johnsen, C. Kvarnemo, E. H. Leder, J. T. Lifjeld, C. E. Ninné, M. Olsson, et al. 2019. Endless forms of sexual selection. *PeerJ* 7:e7988.

Martínez-Ruiz, C., and R. J. Knell. 2017. Sexual selection can both increase and decrease extinction probability: reconciling demographic and evolutionary factors. *J. Anim. Ecol.* 86:117–127.

McDonald, T. K., and S. Yeaman. 2018. Effect of migration and environmental heterogeneity on the maintenance of quantitative genetic variation: a simulation study. *J. Evol. Biol.* 31:1386–1399.

Mead, L. S., and S. J. Arnold. 2004. Quantitative genetic models of sexual selection. *Trends Ecol. Evol.* 19:264–271.

M'Gonigle, L. K., R. Mazzucco, S. P. Otto, and U. Dieckmann. 2012. Sexual selection enables long-term coexistence despite ecological equivalence. *Nature* 484:506–509.

Payne, R. J. H., and D. C. Krakauer. 1997. Sexual selection, space, and speciation. *Evolution* 51:1–9.

Pomiankowski, A. 1987. The costs of choice in sexual selection. *J. Theor. Biol.* 128:195–218.

Pomiankowski, A., and A. P. Møller. 1995. A resolution of the lek paradox. *Proc. R. Soc. B Biol. Sci.* 260:21–29.

Pomiankowski, A., Y. Iwasa, and S. Nee. 1991. The evolution of costly mate preferences I. Fisher and biased mutation. *Evolution* 45:1422–1430.

Ponkshe, A., and J. A. Endler. 2018. Effects of female preference intensity on the permissiveness of sexual trait polymorphisms. *Ecol. Evol.* 8:4518–4524.

Prokuda, A. Y., and D. A. Roff. 2014. The quantitative genetics of sexually selected traits, preferred traits and preference: a review and analysis of the data. *J. Evol. Biol.* 27:2283–2296.

Proulx, S. R. 2001. Female choice via indicator traits easily evolves in the face of recombination and migration. *Evolution* 55:2401–24011.

Radwan, J. 2008. Maintenance of genetic variation in sexual ornaments: a review of the mechanisms. *Genetica* 134:113–127.

Radwan, J., L. Engqvist, and K. Reinhold. 2016. A paradox of genetic variance in epigamic traits: beyond "good genes" view of sexual selection. *Evol. Biol.* 43:267–275.

Reid, J. M., and P. Arcese. 2020. Recent immigrants alter the quantitative genetic architecture of paternity in song sparrows. *Evol. Lett.* 4:124–136.

Reinhold, K. 2004. Modeling a version of the good-genes hypothesis: female choice of locally adapted males. *Org. Divers. Evol.* 4:157–163.

Reznick, D. 2016. Hard and soft selection revisited: how evolution by natural selection works in the real world. *J. Hered.* 107:3–14.

Rowe, L., and D. Houle. 1996. The lek paradox and the capture of genetic variance by condition dependent traits. *Proc. R. Soc. B Biol. Sci.* 263:1415–1421.

Servedio, M. R., and R. Bürger. 2014. The counterintuitive role of sexual selection in species maintenance and speciation. *Proc. Natl. Acad. Sci. USA* 111:8113–8118.

—. 2015. The effects of sexual selection on trait divergence in a peripheral population with gene flow. *Evolution* 69:2648–2661.

Shaw, A. K., and H. Kokko. 2014. Mate finding, Allee effects and selection for sex-biased dispersal. *J. Anim. Ecol.* 83:1256–1267.

Tanaka, Y. 1996. Sexual selection enhances population extinction in a changing environment. *J. Theor. Biol.* 180:197–206.

Tazzyman, S. J., and Y. Iwasa. 2010. Sexual selection can increase the effect of random genetic drift—a quantitative genetic model of polymorphism in *Oophaga pumilio*, the strawberry poison-dart frog. *Evolution* 64:1719–1728.

Tomkins, J. L., J. Radwan, J. S. Kotiaho, and T. Tregenza. 2004. Genic capture and resolving the lek paradox. *Trends Ecol. Evol.* 19:323–328.

Uyeda, J. C., S. J. Arnold, P. A. Hohenlohe, and L. S. Mead. 2009. Drift promotes speciation by sexual selection. *Evolution* 63:583–594.

Wellenreuther, M., E. I. Svensson, and B. Hansson. 2014. Sexual selection and genetic colour polymorphisms in animals. *Mol. Ecol.* 23:5398–5414.

Wiens, J. J., and E. Tuschhoff. 2020. Songs versus colours versus horns: what explains the diversity of sexually selected traits? *Biol. Rev. Camb. Philos. Soc.* 95:847–864.

Wong, B. B. M., and U. Candolin. 2005. How is female mate choice affected by male competition? *Biol. Rev. Camb. Philos. Soc.* 80:559–571.

Zastavniouk, C., L. K. Weir, and D. J. Fraser. 2017. The evolutionary consequences of habitat fragmentation: body morphology and coloration differentiation among brook trout populations of varying size. *Ecol. Evol.* 7:6850–6862.

Associate Editor: M. Dean

Handling Editor: A. McAdam

Supporting Information

Additional supporting information may be found online in the Supporting Information section at the end of the article.

Table S1. Summary of variables and parameter values used in models of coevolution of preference (P) and display (D).

Figure S1. Coevolution of female control trait (FC, random mating) and male display in metapopulations composed of 49 subpopulations under varying levels of dispersal probability over 250,000 generations.

Figure S2. Effect of metapopulation subdivision (number of subpopulations) on the coevolution of a female control trait and male display, given different dispersal probabilities.

Figure S3. Population divergence in female control trait genotype gFC and male display genotype gD (A-B) over 250,000 generations and (C-D) with different levels of metapopulation subdivision (number of subpopulations) as a function of dispersal probability at generation 250,000.

Figure S4. Contribution of dispersal variance (A) and segregating variance (B) to the total additive genetic variance in male display.

Figure S5. Two measures of immigrant maladaptation to the sexually selected environment in metapopulation composed of 49 subpopulations.

Figure S6. Effect of the strength of stabilising natural selection on female preference ($\omega^2_P = 400, 25$; weak and strong respectively) on the coevolution of costly female preference and male display under varying levels of dispersal.

Figure S7. Effect of the strength of stabilising natural selection on female preference ($\omega^2_P = 400, 25$; weak and strong respectively) on population divergence in female preference under varying levels of dispersal.

Figure S8. Effect of weaker stabilising natural selection on male display ($\omega^2_D = 100$) for coevolution of costly female preference and male display under varying levels of dispersal.

Figure S9. Population divergence in female preference genotype gP and male display genotype gD when stabilising natural selection on male display is relaxed ($\omega^2_D = 100$) in metapopulations composed of 49 subpopulations over 250,000 generations.

Figure S10. Coevolution of costly female preference and male display when both positive and negative preferences can evolve (i.e., male display naturally selected optimum $\theta_D = 10$).

Figure S11. Population divergence in female preference genotype gP and male display genotype gD when both positive and negative preferences can evolve (i.e., male display naturally selected optimum $\theta_D = 10$).

Figure S12. Coevolution of costly female preference and male display when the number of loci underlying the traits $L = 100$.

Figure S13. Comparison between $L = 10$ and $L = 100$ (solid and dashed line) on additive genetic variance in male display between generation 100,000 and 250,000.

Figure S14. Population divergence in female preference genotype gP and male display genotype gD when number of loci underlying sexual traits is increased ($L = 100$) in metapopulations composed of 49 subpopulations over 250,000 generations.

Figure S15. Effect of lower mutation rate ($\mu = 5 \times 10^{-6}$ /allele/generation) on the coevolution of costly female preference and male display under varying levels of dispersal.

Figure S16. Population divergence in female preference genotype gP and male display genotype gD under mutation rate $\mu = 5 \times 10^{-6}$ /allele/generation in metapopulations composed of 49 subpopulations over 250,000 generations.

Figure S17. Coevolution of costly female preference and male display in the absence of initial genetic variation in preference and display.

Figure S18. Population divergence in female preference genotype gP and male display genotype gD in metapopulations of 49 subpopulations over 250,000 generations. Simulations started without standing genetic variation for preference and display.

Figure S19. Coevolution of costly female preference and male display in metapopulations composed of 9 subpopulations under varying levels of dispersal over 250,000 generations.

Figure S20. Coevolution of costly female preference and male display in metapopulations composed of 25 subpopulations under varying levels of dispersal over 250,000 generations. Panels.

Figure S21. Coevolution of costly female preference and male display in metapopulations composed of 100 subpopulations under varying levels of dispersal over 250,000 generations.

Figure S22. Coevolution of costly female preference and male display in metapopulations composed of 144 subpopulations under varying levels of dispersal over 250,000 generations.

Figure S23. Population divergence in female preference genotype gP and male display genotype gD in metapopulations under varying levels of metapopulation subdivision (number of subpopulations 9, 25, 100, 144) over 250,000 generations.

Figure S24. Proportion of subpopulations going extinct per metapopulation for different dispersal probabilities (columns) and across levels of spatial subdivision (rows).

Figure S25. Proportion of subpopulations going extinct per metapopulation for different dispersal probabilities (different panels) in metapopulations composed of 49 subpopulations when stabilising natural selection on male display is relaxed ($\omega^2_D = 100$).

Figure S26. Evolutionary trajectories of preference-display across 10,000 generations.

Figure S27. Absolute number of emigrants per subpopulation added-up over a time interval of 1,000 generations for different dispersal probabilities: A) $d = 5 \times 10^{-5}$; B) $d = 5 \times 10^{-4}$; C) $d = 5 \times 10^{-3}$ and D) $d = 5 \times 10^{-2}$.